World Academy of Science, Engineering and Technology
International Journal of Aerospace and Mechanical Engineering
Vol:11, No:12, 2017

Increase of Sensitivity in 3D Suspended Polymeric Microfluidic Platform through Lateral Misalignment

Ehsan Yazdanpanah Moghadam, Muthukumaran Packirisamy

***Abstract*—**In the present study, a design of the suspended polymeric microfluidic platform is introduced that is fabricated with three polymeric layers. Changing the microchannel plane to be perpendicular to microcantilever plane, drastically decreases moment of inertia in that direction. In addition, the platform is made of polymer (around five orders of magnitude less compared to silicon). It causes significant increase in the sensitivity of the cantilever deflection. Next, although the dimensions of this platform are constant, by misaligning the embedded microchannels laterally in the suspended microfluidic platform, the sensitivity can be highly increased. The investigation is studied on four fluids including water, seawater, milk, and blood for flow ranges from low rate of 5 to 70 µl/min to obtain the best design with the highest sensitivity. The best design in this study shows the sensitivity increases around 50% for water, seawater, milk, and blood at the flow rate of 70 µl/min by just misaligning the embedded microchannels in the suspended polymeric microfluidic platform.

***Keywords*—**Microfluidic, biosensor, MEMS.

I. Introduction

ONE of the most applicable sensors that have been adopted based on the atomic force microscope (AFM) is cantilever-based sensor, and according to the application, it can work in either dynamic or static modes [1]-[3]. Chemical, biophysical, or physical phenomena cause alterations in surface stress, and this deflection can be transformed to the mechanical signal through bending of the cantilever [4]-[6]. For monitoring the beam deflection, laser beam-based deflection method has been introduced to determine the rate of bending in a beam. In addition, their ultra-sensitive position sensitive detectors (PSDs) and their readout technique allow detecting sub angstrom changes in the deflection [7]. One of the most important concerns of physicians and scientists during this century is deciphering the mechanism of the changes that happen during cancer metastasis. In view of the fact that cancer cells are not always embedded in the extracellular matrix or endothelial cell–cell junctions and sometimes they can detach from their tissues travel throughout the vessels to the other parts of the body [8]. This is the stage when the tumor starts to become metastatic and cancer cells experience lots of biochemical and cyto-skeletal modifications that drive them to the invasive cells [9], [10]. Therefore, the physical properties of the cells, including their viscoelastic and frictional features can change during this stage [8]. So far, many different strategies according to these mechanical properties such as micropipette aspiration [11], [12], atomic force microscopy (cantilever-based sensor) [13], microrheology [14] and the especially microfluidic technique [15], [16] have been developed in order to measure these biomechanical properties of cells. In 2002, Marie et al. utilized micro-cantilever technology for specific detection of biomarkers. Using this strategy, they achieved to detect a specific DNA target via measuring the change in the deflection of micro-cantilever beam [17]. Following that, Cherian et al. [18] used the same strategy to sensitive and specific heavy metal ions that had an affinity with functionalized protein. Shih et al. [19] combined micro-cantilever method with the powerful piezoelectric technology for designing biosensors, and as a result, the quality and the sensitivity of the sensor were highly improved. This technique has also been reported for susceptible determination of biophysical properties of cancerous cells, which claimed that such cells are highly efficient to squeeze through tight capillary due to the fact that their deformability and friction are increased and decreased respectively during their transformation from normal cells to cancerous cells [8].

In this work, we develop a sensitive multilayer microcantilever. The microfluidic channels are designed inside the cantilever was fabricated from polymer. By tuning the microchannels of this micro-cantilever in constant geometry, the sensitivity of this sensor is highly improved. The highly sensitivity is obtained just by misaligning microchannels that are embedded in the suspended microfluidic platform.

II. Result and Discussion

The microcantilever simulated in this study is shown in Fig. 1. As indicated in Fig. 1, this device has three layers that are made of polydimethylsiloxane (PDMS). First microchannel, nozzle, and second microchannel are embedded in top, middle, and bottom layers of the cantilever, respectively. The nozzle at the tip of the cantilever connects the top channel to the bottom channel (Fig. 1). Fig. 1 shows the fluid enters the input port that is connected the top channel and then passes through the embedded nozzle in the middle layer and goes through the second channel in the third layer and then exits from the output port. As observed in Fig. 1 (b), the two channels at the top layer and the bottom layer are at different levels, but parallel. In this project, we increase the distance between two channels laterally in opposite direction to observe the deflection of the microcantilever tip. It means that if the front view is taken, the distance of each channel increases

Ehsan Yazdanpanah Moghadam is PhD Candidate of Concordia University, Montreal, Canada (corresponding author, phone: (+1) 514 992 5002, e-mail: e.yazdan.m@gmail.com).

Muthukumaran Packirisamy is Professor of Mechanical engineering Department of Concordia University, Montreal, Canada (phone: (+1) 514 8482, e-mail: mpackir@encs.concordia.ca).

horizontally from each other with respect to the nozzle center.

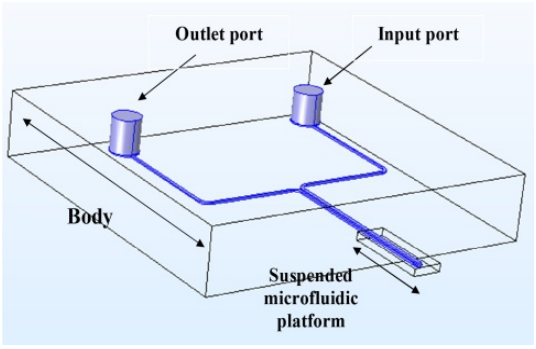

(a)

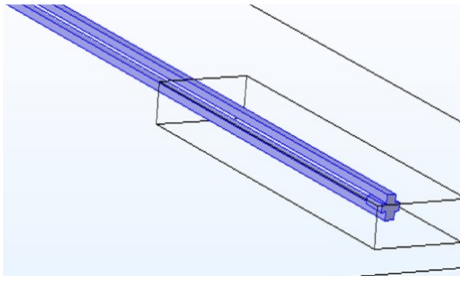

(b)

Fig. 1 Geometrical configure of the microcantilever design 1 (a) 3D view (b) 3D view from the embedded channels and the nozzle in the suspended polymeric microchannel platform in COMSOL

TABLE I
PROPERTIES OF FLUIDS AT 20^{0C}

Fluid	Density (kg/m^3)	Dynamic viscosity (Pa. s)
Water	1002	1.002x10^{-3}
Seawater	1028	1.08x10^{-3}
Milk	1035	1.13x10^{-3}
Blood	1060	4x10^{-3}

The width and height of the cantilever are 2 and 6 mm, respectively. This innovative resonator has three layers of PDMS where the first layer thickness is 200 µm, the second layer is 100 µm, and last layer is 200 µm. The width and thickness of embedded channels in the cantilever are 200 and 100 µm, respectively. The diameter of input and output port is 2 mm. The width and length of nozzle in the second layer are 400 µm. The microcantilever deflection is investigated for four designs are named design 1, design 2, design 3, and design 4. The design 1 is base, but for others, the top channel moves to the right side and the bottom channel moves to the left side horizontally. This distance between the channels at each design increases, although the nozzle at the central layer is constant. Fig. 1 indicates design 1, if the front view is taken (Fig. 3 (a)); the distance of the channel center from the nozzle center is zero. In design 2, each channel becomes far from the center that this distance is 50 µm. In design 3, this distance is 100 µm. Finally, in design 4, it reaches 200 µm.

The range of the chosen flow rates starts from 5 to 70 microliters per minute (µl/min). Table I shows the fluids applied and their basic properties at 20 °C. These fluids are water, seawater, milk, and blood. In order to investigate biocompatibility of the microcantilever, we selected the blood as an applied fluid in this report.

A. Mesh Independence and Simulation Validation

The simulation of whole geometry in 3D modeling is computationally expensive. On the other hand, the body of the microcantilever does not affect the cantilever deflection, so just the suspended microcantilever is simulated instead of the whole geometry.

In COMSOL simulation, the physics of Fluid-Solid interaction was selected, and the flow rate was assumed to be incompressible. The region that fluid enters to the suspended channel is fully developed, so entrance distance is zero in the simulation. Flow in the channel is laminar. To valid simulation accuracy of the solution, we selected different element sizes: 4404, 8449, 13002, 21770, and 49712 (Fig. 2 (a)). The applied fluid at different element sizes is water, and the flow rate is set 5 µl /min. Fig. 2 shows after the element size of 13002, the slope of deflection difference decreases, so that, at element sizes of 21770 and 49712, the deflection reaches stability. Therefore, in our simulation, the element size of 21770 is chosen.

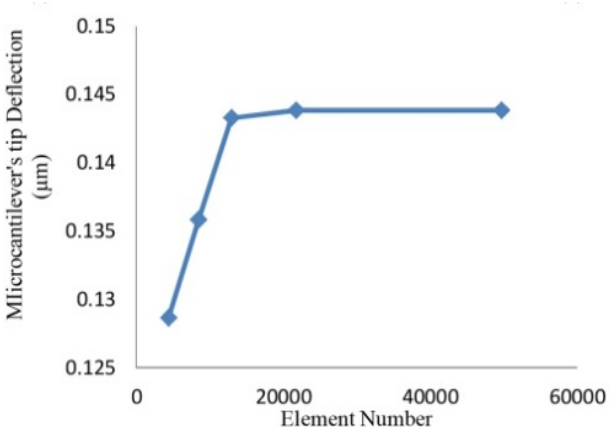

Fig. 2 Simulation samples in COMSOL to check the mesh independence for flow rate of 5 µl /min in design 1 of the microcantilever for water

B. Proposed Designs

1. Design 1

In design 1, Figs. 3 (a) and (b) shows the position of two channels in the cantilever. As the front view is taken (Fig. 3 (a)), the center of two channels is set at the center of the nozzle. As shown in Figs. 3 (c) and (d), the cantilever deflection for blood is plotted separately from water, seawater, milk. Because the deflection of the cantilever tip for blood is much higher, compared to other the applied fluids.

Figs. 3 (c) and (d) illustrate that the cantilever deflection at 5 µl/min is almost 1.44 µm. By increasing the flow rate, the deflection rises and reaches 2.075 µm at 70 µl/min. Because, at higher flow rate, more volume of the water flows through the cantilever, and subsequently, the cantilever deflection

increases. This upward trend for seawater, milk, and blood is also the same. This increase of the tip displacement for seawater, milk, blood is higher in comparison with water at each flow rate, since their density is greater than water. It means that, by rising the density of fluid, dynamic viscosity increases. So, the shear stress between inside the channels and fluid increases, that leads to the rise of the cantilever deflection.

2. Design 2

In the second design, a lateral misalignment between the top channel and the bottom channel is made. As demonstrated in Fig. 4 (a), the top channel is shifted to the left side 50 µm, and the bottom channel is moved to the right side 50 µm laterally with respect to the nozzle center.

As water in design 2 is used as a fluid which goes through the suspended cantilever, the deflection of the microcantilever tip for water at 5 µl/min reaches 0.152 µm. It is a 6% increase in comparison with design 1 at the same flow rate. By increasing flow rate to 70 µl/min, this increase reaches around 0.22 µm; it is an 8% increase, compared to the design 1 at the same flow rate. The same increase for the other fluids can be seen.

3. Design 3

Figs. 5 (a) and (b) indicates in design 3 that the distance of each channel center from the nozzle center reaches to 100 µm. Fig. 5 (c) illustrates that this design is more sensitive in comparison with the design 1 and 2. For example, at the flow rate 5 µl/min for milk in the design 3, the displacement of the microcantilever tip is roughly 0.18 µm, while, at the same flow rate for design 2, it is around 0.16 µm. This sensitivity for other applied fluids rises with the increase of the flow rate.

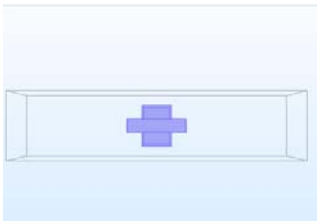

(a)

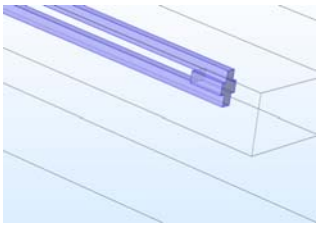

(b)

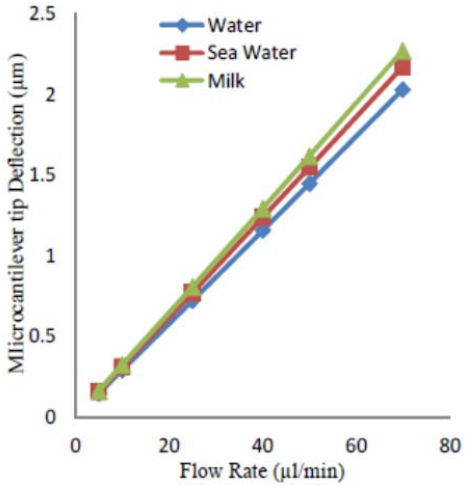

(c)

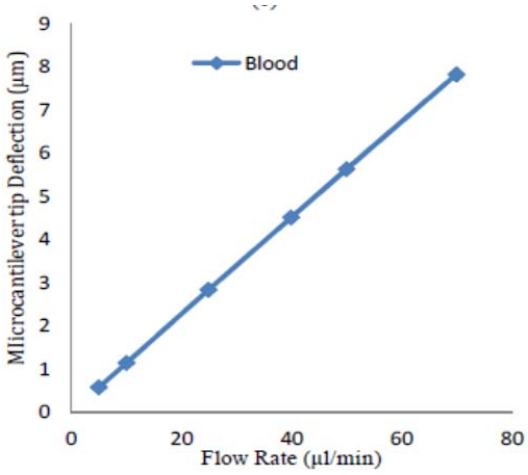

(d)

Fig. 3 Geometrical configuration of channels in design 1 from (a) front view (b) 3D view from the cantilever tip (c) maximum reflection for water, seawater, and milk (d) maximum deflection for blood

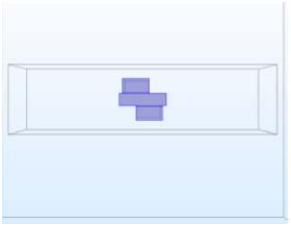

(a)

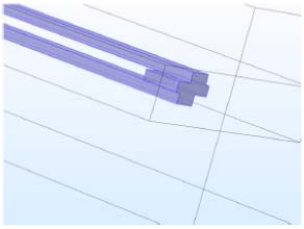

(b)

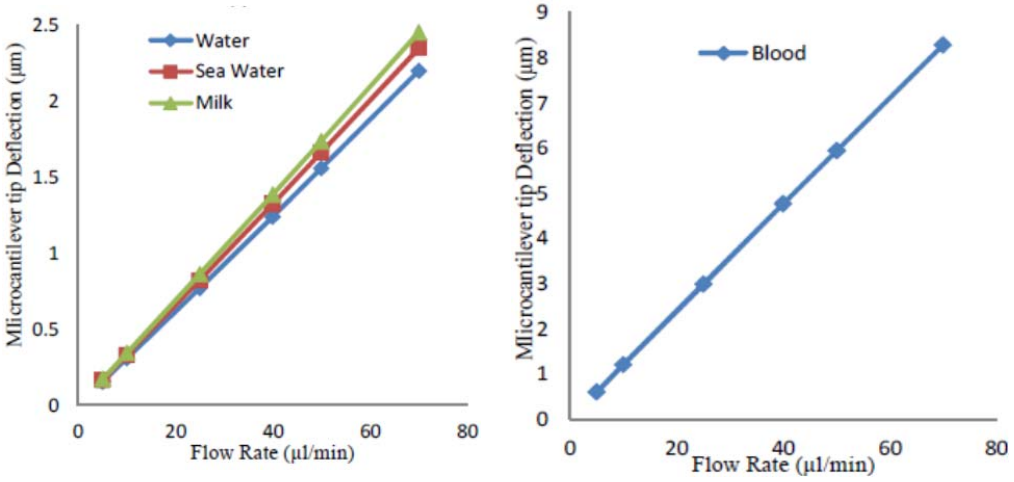

(c) (d)

Fig. 4 Geometrical configuration of channels in design 2 from (a) front view (b) 3D view from the cantilever tip (c) maximum reflection of water, seawater, and milk (d) maximum deflection for blood

(a) (b)

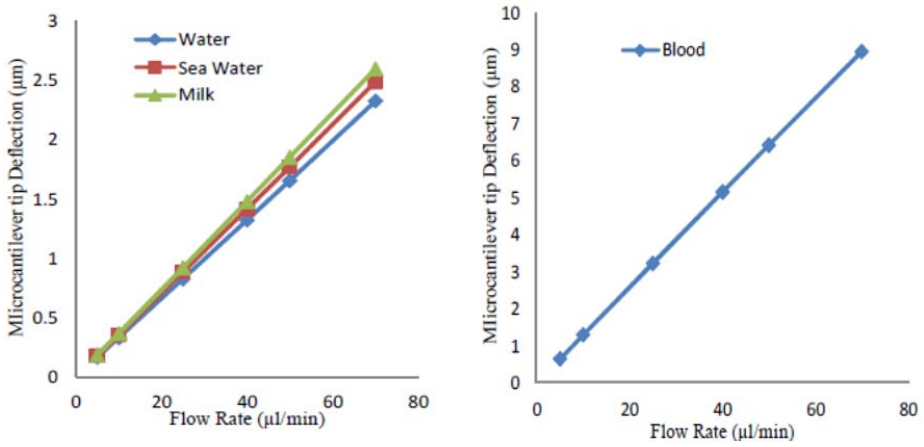

(c) (d)

Fig. 5 Geometrical configuration of channels in design 3 from (a) front view (b) 3D view from the cantilever tip (c) maximum reflection for water, seawater, and milk (d) maximum deflection for blood

(a) (b)

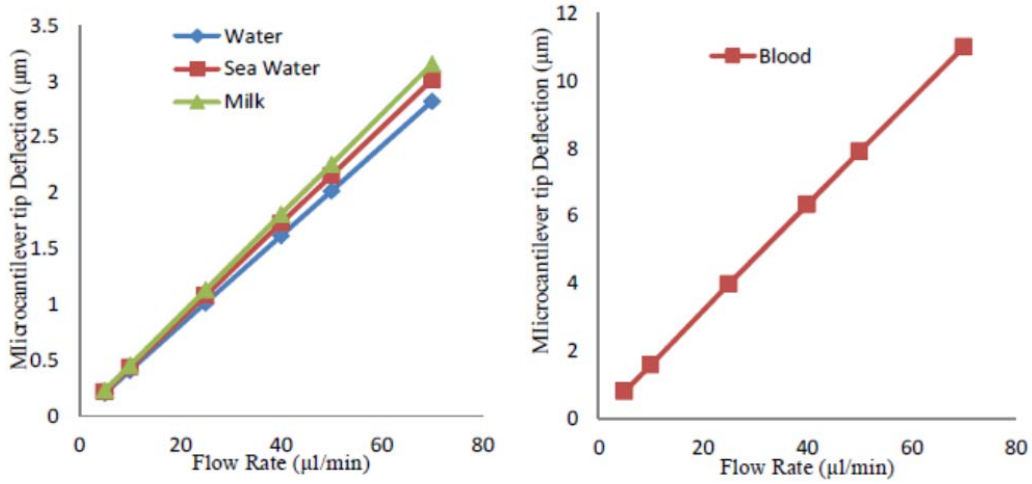

(c) (d)

Fig. 6 Geometrical configuration of channels in design 4 from (a) front view (b) 3D view from the cantilever tip (c) maximum reflection of water, seawater, and milk (d) maximum deflection for blood

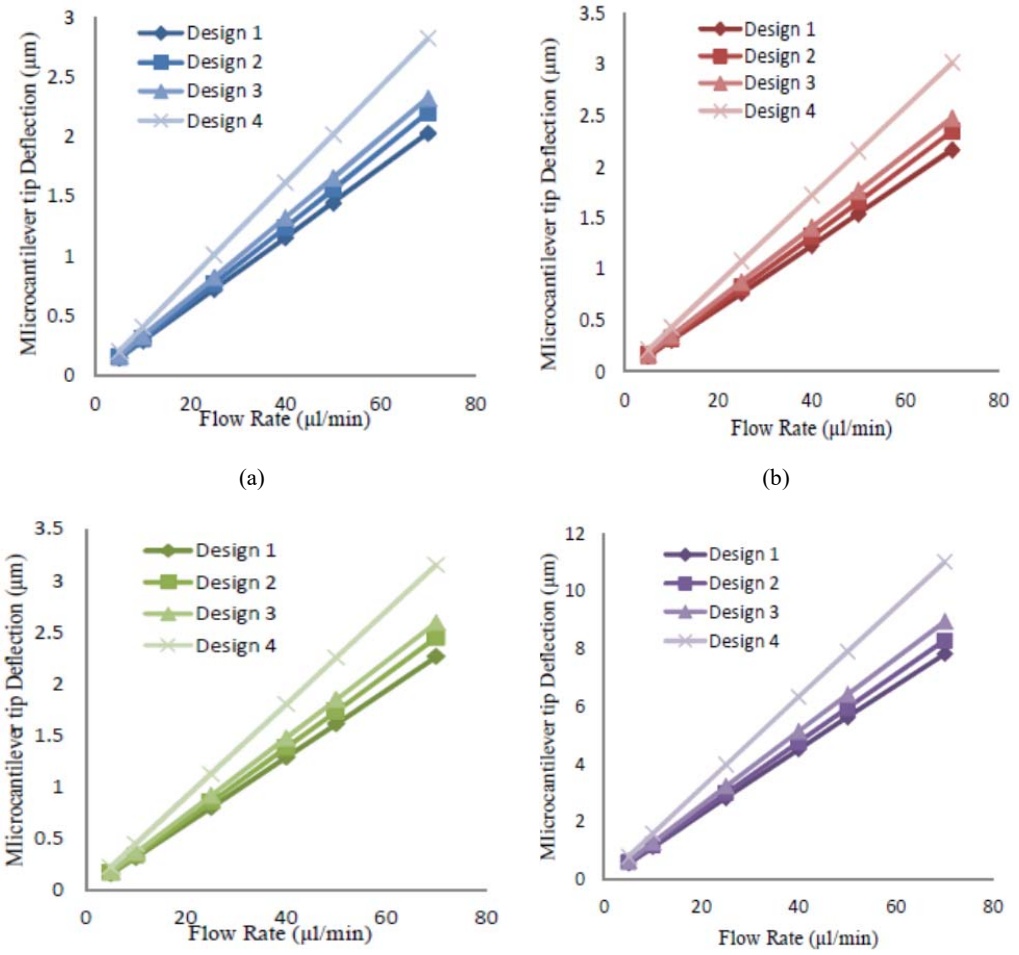

(a) (b)

(c) (d)

Fig. 7 Variation of the cantilever tip deflection for the four designs for (a) water (b) seawater (c) milk (d) blood

4. Design 4

Figs. 6 (a) and (b) indicate that the distance between the top and bottom channel horizontally increases more that design 1, 2, and 3. The distance of each channel center reaches 200 µm with respect to the nozzle center. Fig. 6 (c) shows, in design 4, that the increase of the microcantilever deflection continues

for the applied fluids, compared to design 1, 2, and 3 at each flow rate. For instance, at 70 µl/min, the cantilever deflection in design 3 is around 9.5 µm, while it increases to almost 12 µm in design 4 at the same flow rate.

C. Comparison Designs

In this section, we compare the displacement of the microcantilever tip in the different designs for the four applied fluids. Figs. 7 (a)-(d) demonstrates when the deflection of the microcantilever tip in the design 4 is compared with design 1, 2, and 3 at each flow rate in the different fluids, it is clear that the deflection of the cantilever tip in design 4 is the highest. This misalignment proposed could increase the sensitivity of the microcantilever up to approximately 50% for the applied fluids at the flow rate of 70 µl/min. In addition, the variation range of the cantilever deflection for design 4 between 5 and 70 µl/min is higher than other designs. For example, the cantilever deflection for milk in design 1 changed from 0.16 µm at 5 µl/min to 2.27 µm at 70 µl/min, while, in design 4 for same fluid, the deflection varies between 0.226 µm to 3.16 µm. It means a 40% increase in the deflection range just by changing design from 1 to 4. In fact, by increasing the lateral distance of the channels, the area of passing fluid from the top channel to the nozzle and the nozzle to the bottom channel decreases, which leads to higher velocity and the shear stress in the design 4 between the channels and the nozzle, compared to design 1, 2, and 3. As a result, the design 4 is chosen as the most sensitive design among the proposed designs.

III. Conclusion

The current research investigated the design of a 3D suspended polymeric microfluidic platform. In order to increase its sensitivity, first this platform was made in three layers to increase the momentum and then instead of silicon, polymer was applied (around five orders of magnitude less than silicon) for fabrication. Moreover, to optimize the sensitivity of this platform, by misaligning the channels laterally, the sensitivity of microcantilever was increased up to 50% for water, seawater, milk, and blood at the flow rate of 70 µm/min although all the dimensions of this sensor were constant. This misalignment was proposed for four designs for water, seawater, milk, and blood from low flow of 5 to 70 µl/min. As expected, by increasing flow rate through microchannels, the displacement of the microcantilever tip increases. The same increase trend was observed, when the density and dynamic viscosity of the applied fluids rise.

References

[1] Watari, Moyu, et al. "Investigating the molecular mechanisms of in-plane mechanochemistry on cantilever arrays." Journal of the American Chemical Society 129.3 (2007): 601-609.
[2] Huber, François, et al. "Label free analysis of transcription factors using microcantilever arrays." Biosensors and Bioelectronics 21.8 (2006): 1599-1605.
[3] Mertens, Johann, et al. "Label-free detection of DNA hybridization based on hydration-induced tension in nucleic acid films." Nature nanotechnology 3.5 (2008): 301-307.
[4] Wu, Guanghua, et al. "Origin of nanomechanical cantilever motion generated from biomolecular interactions." Proceedings of the National Academy of Sciences 98.4 (2001): 1560-1564.
[5] Gimzewski, J. K., et al. "Observation of a chemical reaction using a micromechanical sensor." Chemical Physics Letters 217.5-6 (1994): 589-594.
[6] Berger, R., et al. "Thermal analysis using a micromechanical calorimeter." Applied Physics Letters 69.1 (1996): 40-42.
[7] Mishra, Rohit, Wilfried Grange, and Martin Hegner. "Rapid and reliable calibration of laser beam deflection system for microcantilever-based sensor setups." Journal of Sensors 2012 (2011).
[8] Byun, Sangwon, et al. "Characterizing deformability and surface friction of cancer cells." Proceedings of the National Academy of Sciences 110.19 (2013): 7580-7585.
[9] Wirtz, Denis, Konstantinos Konstantopoulos, and Peter C. Searson. "The physics of cancer: the role of physical interactions and mechanical forces in metastasis." Nature Reviews Cancer 11.7 (2011): 512-522.
[10] Kalluri, Raghu, and Robert A. Weinberg. "The basics of epithelial-mesenchymal transition." The Journal of clinical investigation 119.6 (2009): 1420-1428.
[11] Drury, Jeanie L., and Micah Dembo. "Aspiration of human neutrophils: effects of shear thinning and cortical dissipation." Biophysical Journal 81.6 (2001): 3166-3177.
[12] Hochmuth, Robert M. "Micropipette aspiration of living cells." Journal of biomechanics 33.1 (2000): 15-22.
[13] Hansma, Helen G., and Jan H. Hoh. "Biomolecular imaging with the atomic force microscope." Annual review of biophysics and biomolecular structure 23.1 (1994): 115-140.
[14] Bausch, Andreas R., et al. "Local measurements of viscoelastic parameters of adherent cell surfaces by magnetic bead microrheometry." Biophysical journal 75.4 (1998): 2038-2049.
[15] Adamo, Andrea, et al. "Microfluidic-based assessment of cell deformability." Analytical chemistry 84.15 (2012): 6438.
[16] Chen, Jian, et al. "Classification of cell types using a microfluidic device for mechanical and electrical measurement on single cells." Lab on a Chip 11.18 (2011): 3174-3181.
[17] Marie, Rodolphe, et al. "Adsorption kinetics and mechanical properties of thiol-modified DNA-oligos on gold investigated by microcantilever sensors." Ultramicroscopy 91.1 (2002): 29-36.
[18] Cherian, Suman, et al. "Detection of heavy metal ions using protein-functionalized microcantilever sensors." Biosensors and Bioelectronics 19.5 (2003): 411-416.
[19] follo, Wan Y., et al. "Piezoelectric microcantilever sensors for biosensing." U.S. Patent No. 8,927,259. 6 Jan. 2015.